

heat and vapor mass fluxes per unit volume of medium; ω , parameter defined in (16). Indices: 0, 1, continuous and dispersed phases, respectively; *, quantities perturbed by test particle; °, parameters of medium when there is no phase transition.

LITERATURE CITED

1. Yu. A. Buevich, Yu. A. Korneev, and I. N. Shchelchkova, *Inzh.-Fiz. Zh.*, No. 6 (1976).
2. Yu. A. Buevich and Yu. A. Korneev, *Inzh.-Fiz. Zh.*, 31, No. 1 (1976).
3. Yu. A. Buevich and Yu. A. Korneev, *Inzh.-Fiz. Zh.*, 31, No. 4 (1976).
4. V. A. Borodulya and Yu. A. Buevich, *Inzh.-Fiz. Zh.*, 32, No. 2 (1977).
5. Yu. A. Buevich and Yu. A. Korneev, *Zh. Prikl. Mekh. Tekh. Fiz.*, No. 4, 79 (1974).

RATE OF BUBBLE RISE IN A NONUNIFORM FLUIDIZED BED

A. I. Tamarin, Yu. S. Teplitskii,
and Yu. E. Livshits

UDC 532.546

The dimensions and rate of rise of bubbles in a column 700 mm in diameter were determined experimentally. On the basis of a two-phase model, a calculated correlation was obtained which related the relative velocity of a gas bubble to its diameter.

At the present time, the problem of the rise of a single artificial bubble in a uniform fluidized bed has been studied in some detail in the literature and the dependence of its velocity on diameter obtained [3]:

$$v_b = k \sqrt{g \frac{1}{2} D_b}, \quad (1)$$

where $0.8 \leq k \leq 1.2$.

In a nonuniform fluidized bed, coalescence of bubbles occurs and there is only fragmentary data on the rates of rise and dimensions of gaseous nonuniformities averaged across the fluidized bed [4-6, 9, 10]. There is almost no data for columns of large diameter [11]. At the same time, this information is of great interest for the design of commercial equipment.

The present paper is aimed at the problems of obtaining information about the quantities v_B and D_B in a column 700 mm in diameter and of unifying the known experimental data.

The following correlation for the vertical size of a bubble was obtained [8] for equipment of different sizes ($100 \text{ mm} \leq D \leq 700 \text{ mm}$):

$$D_h = \frac{1.3}{g^{1/3}} [(u - u_0) h]^{2/3}, \quad (2)$$

and is connected to bubble diameter through the relation [13] $D_h = 0.7D_B$. Equation (2) is valid for small particles ($70 < d < 400 \mu$) and uniform gas distribution.

For similar conditions a relationship was found [2] for expansion of the bed:

$$p - 1 = 0.7 \left(\frac{H_0}{D} \right)^{1/2} Fr^{1/3} \quad (3)$$

for $D = 100-700 \text{ mm}$ and $0.5 < H_0/D < 2$.

A. V. Lykov Institute of Heat and Mass Transfer, Academy of Sciences of the Belorussian SSR, Minsk. Translated from *Inzhenerno-Fizicheski Zhurnal*, Vol. 32, No. 4, pp. 632-636, April, 1977. Original article submitted March 15, 1976.

This material is protected by copyright registered in the name of Plenum Publishing Corporation, 227 West 17th Street, New York, N.Y. 10011. No part of this publication may be reproduced, stored in a retrieval system, or transmitted, in any form or by any means, electronic, mechanical, photocopying, microfilming, recording or otherwise, without written permission of the publisher. A copy of this article is available from the publisher for \$7.50.

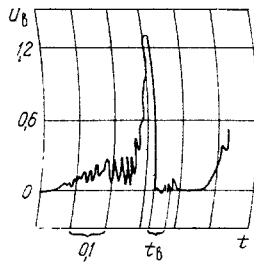


Fig. 1

Fig. 1. Sample of typical probe signal: u_B , m/sec; t , sec.

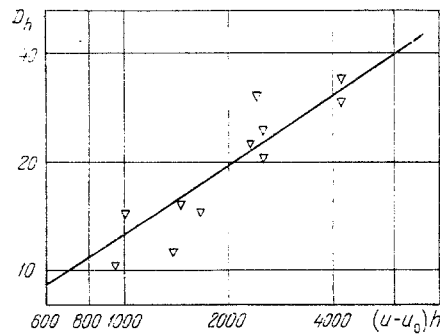


Fig. 2

Fig. 2. Dependence of gas-bubble height D_h , cm, on the quantity $(u - u_0)h$, cm^2/sec .

Using the well-known relation [3]

$$p - 1 = \frac{u - u_0}{v_B}, \quad (4)$$

we obtain the following relation from Eqs. (2), (3) and (2)-(4):

$$v_B = k_1 \sqrt{gD_B}, \quad k_1 = 1.4 \left(\frac{D}{H_0} \right)^{1/2} \quad (5)$$

for $D = 100-700$ mm.

The relation (5) establishes a connection between the kinetic energy of the relative motion of a gas bubble and the potential energy of the emulsion phase in the gravitational field. It is similar to Eq. (1). In this case, the diameter D_B of the gas bubble appears with a correction which reflects the geometric characteristic of the system H_0/D and which takes into account the nature of the interactions between bubbles within the volume of the fluidized bed. It is clear from Eq. (5) that real bubbles may move markedly more rapidly in a nonuniform bed than the artificial bubbles of Eq. (1).

Special experiments were performed in order to refine relation (5). The experiments were performed in a column 700 mm in diameter. The gas-distribution grid was made of two perforated sheets with holes 10 mm in diameter. The 25-mm spacing between holes provided a useful cross section of 11.5%. A layer of felt 9 mm thick was clamped between the perforated sheets. Polydisperse quartz sand with a mean particle diameter of 0.23 mm ($u_0 = 4.6$ cm/sec, $\epsilon_0 = 0.45$) was used as the dispersed material. The quantities u_0 and ϵ_0 were determined by smooth reduction of gas velocity using standard techniques. The height H_0 of the motionless charge was 50 and 90 cm. Fluidization was accomplished with air at $t = 20^\circ\text{C}$. Air flow was measured to better than 3% by means of a diaphragm and differential manometer.

A sensing dynamometer, the operating principles of which were described in [7], was used. It was a flexible strip of phosphor bronze with a rigid spindle at the end. A plastic sphere (5.5 mm in diameter) was mounted on the end of the spindle. The force acting on the sphere was measured with two strain gauges glued to the elastic strip and connected to a TA-5 strain-gauge test stand. The output signal from the test stand was recorded on a strip chart by an H-327-3 high-speed recorder. The sensing element was calibrated by means of a static load suspended from the sphere. The force acting on the sensing element was determined to 5% in the frequency range from 0 to 50 Hz. The sensing element was installed at the upper boundary of the motionless bed at distances of 50 and 90 cm, respectively, from the gas-distribution grid. The range of fluidization numbers for the sand was 6-12.

Dynamic calibration of the sensing element was performed by means of cinematography in a flat column 240×35 mm in cross section. A signal from the sensing element was recorded at the time of passage of the base of a bubble and its velocity determined by cinematography. The error of the dynamic calibration was no more than 5%.

The form of a typical signal produced by the recorder during the time a bubble passed the probe is shown in Fig. 1. It is clear from the figure that the signal is zero during the

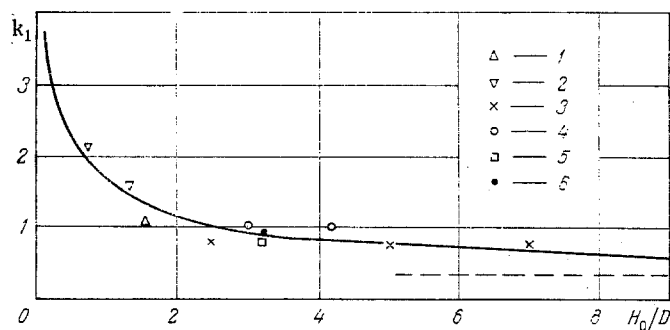


Fig. 3. Dependence of the coefficient $k_1 = v_B / \sqrt{gD_h}$ on the geometric characteristic H_0/D of the bed: 1, 2) our data for columns 300 and 700 mm in diameter, respectively; 3) [5] ($D = 100$ mm, $u_0 = 2.8$ cm/sec); 4) [6] ($D = 75$ mm, $D_{eq} = 100$ mm, $u_0 = 2.4$ cm/sec); 5) [12] ($D = 150$ mm, $d = 100$ μ , $u_0 = 1.1$ cm/sec); 6) [1] ($D = 100$ mm, three fractions of electrically conducting coke with $d = 86, 154,$ and 344 μ).

time t_B when the bubble passes by the sphere of the probe but increases sharply at the time when the base of the bubble impinges on the probe. The length of the zero signal and the height of the spike after the bubble (base of the bubble) were measured on the strip chart. Knowing the chart speed, the time taken by the bubble in passing the sensing element was then determined. Using the static and dynamic calibrations, the velocity of the base of the bubble, which was identified with the velocity \bar{u}_B of the bubble itself, was determined from the height of the spike following the bubble. The height of the bubble was determined from the relation $h_B = \bar{u}_B t_B$. The quantities u_B and D_h were determined by averaging the quantities \bar{u}_B and h_B respectively obtained in each individual case.

It is clear from Fig. 2 that the experimental data is approximated by Eq. (2) with a standard deviation of 15%. Thus the experiments showed that Eq. (2) also remains valid for higher values of the quantity $(u - u_0)h$: $2000 \leq (u - u_0)h \leq 4000$ cm²/sec.

In order to reveal the connection between the bubble height D_h averaged across the bed and the averaged velocity v_B , and also to take into account the effect of the geometric factor H_0/D , the experimental data consistent with Eq. (5) were plotted in logarithmic coordinates: The bubble height was plotted on the abscissa and the quantity $v_B / (D/H_0)^{1/2}$, on the ordinate. The experimental points were correlated with the following equation,

$$v_B = 1.76 \left(\frac{D}{H_0} \right)^{1/2} \sqrt{gD_h} \quad (6)$$

with a standard deviation of 25%.

Plotted in Fig. 3 is the dependence of the coefficient $k_1 = v_B / \sqrt{gD_h}$ on the geometric characteristic of the bed in units of H_0/D according to the theoretical relation (5) (solid line); also plotted are values of k_1 for our experiments and data of other investigators pertaining to nonuniform fluidization [1, 5, 6, 12] and also pertaining to the piston mode [4], for which the value $k_1 = 0.35$ is represented by the dashed line. Plotted in the same figure are data for a sand bed ($u_0 = 4.5$ cm/sec, $\epsilon_0 = 0.45$) in a 300-mm column obtained in the experiments described in [8].

It is clear from Fig. 3 that Eq. (5) approximates rather well (with a standard deviation of 10%) the experimental data obtained over a broad range of H_0/D : $0.7 < H_0/D < 7$.

In conclusion, we point out that the following relation obtained from Eqs. (2) and (5),

$$v_B = 1.9 \left(\frac{D}{H_0} \right)^{1/2} [g(u - u_0)h]^{1/3}, \quad (7)$$

can be recommended for calculating the relative rate of bubble rise averaged across a fluidized bed for $D = 100$ – 700 mm and $70 < d < 400$ μ . Note that Eq. (7) is valid for uniform gas distribution.

NOTATION

D_B , mean bubble diameter across the bed; D , column diameter; k, k_1, k_2 , dimensionless coefficients; g , gravitational acceleration; u, u_0 , velocity of filtration and velocity at initiation of fluidization; H, H_0 , height of bed and height of motionless bed; h , vertical height above gas-distribution grid; $p = H/H_0$, expansion of bed; $Fr = (u - u_0)^2/gH_0$, Froude number; u_B, v_B, \bar{v}_B , absolute rate of bubble rise, relative rate of bubble rise, and relative rate of bubble rise averaged across the bed; \bar{u}_B, \bar{v}_B , local values of bubble velocities; d , diameter of solid particles; ϵ_0 , bed porosity at initiation of fluidization.

LITERATURE CITED

1. W. H. Park, W. K. Kang, C. E. Capes, and G. L. Osberg, *Chem. Eng.* 24, No. 5 (1969).
2. A. I. Tamarin and Yu. S. Teplitskii, *Inzh.-Fiz. Zh.*, 32, No. 3 (1977).
3. J. F. Davidson and D. Harrison, *Fluidised Particles*, Cambridge University Press (1963).
4. J. F. Davidson and D. Harrison (editors), *Fluidization*, Academic Press (1971).
5. R. Toei, R. Matsuno, H. Kojima, Y. Nagai, K. Nakagawa, and S. Yu, Reprint from the Memoirs of the Faculty of Engineering, Kyoto University, Vol. 27, Kyoto, Japan, October (1965), p. 4.
6. H. Kobayashi, F. Arai, and T. Chiba, *Kagaku Kogaku*, 29, 859 (1965).
7. A. I. Tamarin, I. Z. Mats, and G. G. Tyukhai, in: *Heat and Mass Transfer* [in Russian], Vol. 5, Minsk (1968).
8. A. I. Tamarin, Yu. S. Teplitskii, and Yu. E. Livshits, *Inzh.-Fiz. Zh.*, 31, No. 2 (1976).
9. K. Godart and G. F. Richardson, *Chem. Eng. Sci.*, 24, No. 4 (1969).
10. M. Tomita and T. Adachi, *J. Chem. Eng. Japan*, 6, No. 2 (1973).
11. A. Whitehead and A. D. Young, in: *Proceedings of the International Symposium on Fluidization*, Eindhoven, Netherlands, Amsterdam University Press (1967), p. 284.
12. J. M. Burgess and P. N. Calderbank, *Chem. Eng. Sci.*, 30, 1511 (1975).
13. D. Geldart, *Powder Technol.*, 6, No. 4 (1972).

CALCULATION OF CHARACTERISTICS OF A DIRECT-CURRENT

ARGON ARC

A. S. Sergienko and G. A. Fokov

UDC 533.9.082.15

The radial temperature profile of a cylindrical argon arc is calculated by a method based on an elliptical approximation of the function $\sigma(S)$.

Article [1] presented the results of a study of static volt-ampere characteristics of a dc argon arc burning in a cylindrical channel formed by a set of water-cooled electrically neutral copper sections with inner diameter of $d = 6$ mm. The current varied from 30 to 110 A at an argon flow rate of $G = 0.03$ g/sec.

For various practical applications it is important to theoretically calculate the temperature distribution over the section of the arc conductive channel. If we consider that the electrical energy introduced into a unit volume of cylindrically symmetric positive arc column is absorbed by the channel wall solely due to thermal conductivity, then the energy balance equation will have the form [2]

$$\sigma E^2 + \frac{1}{r} \frac{d}{dr} \left(r \lambda \frac{dT}{dr} \right) = 0. \quad (1)$$

A. V. Lykov Institute of Heat and Mass Transfer, Academy of Sciences of the Belorussian SSR, Minsk. Translated from *Inzhenerno-Fizicheskii Zhurnal*, Vol. 32, No. 4, pp. 637-642, April, 1977. Original article submitted December 15, 1975.

This material is protected by copyright registered in the name of Plenum Publishing Corporation, 227 West 17th Street, New York, N. Y. 10011. No part of this publication may be reproduced, stored in a retrieval system, or transmitted, in any form or by any means, electronic, mechanical, photocopying, microfilming, recording or otherwise, without written permission of the publisher. A copy of this article is available from the publisher for \$7.50.